



Bio-synthesised nanoparticles employment for eliminating metals from wastewater via implementation of a three level Box-Behnken technique

P. Jyolsna¹ · V. Gowthami¹ · A. Hajeera Aseen¹

Received: 15 July 2024 / Accepted: 3 January 2025 / Published online: 27 January 2025
© The Author(s) 2025

Abstract

The objective of the present study is to optimise the removal of metals such as aluminium, zinc, and copper from industrial wastewater using green-synthesised nanoadsorbents. To achieve this, the Box–Behnken experimental design and response surface methodology will be employed. We used inductively coupled plasma mass spectrometry to analyse the metals present in the wastewater. A three-factor, three-stage Box–Behnken design was used to maximise the removal of these metals from aqueous solution. This involved response surface modelling and quadratic programming based on 17 different experimental data from a batch study. The study focused on three independent variables: pH, contact time, and adsorbent amount. The nanoadsorbents were prepared using a combination of *Citrus X sinensis* peel and *Musa Cavendish* peel extract, which served as the reducing agents, to produce a combined peel extract-silver nanoparticle product. Field emission scanning electron microscopy imaging and UV–visible spectroscopic analysis unequivocally demonstrated the presence of nanoparticles, with a surface plasmon resonance at 438 nm. The optimal values of the selected variables were determined by solving the quadratic regression model and analysing the contour plots of the reaction surface. At the experimental conditions of pH = 5, contact time = 92.5 min, and adsorbent dosage = 0.1 g/L, the recovery efficiency of Al, Cu, and Zn was significantly reduced. The optimised parameters were successfully applied to wastewater collected, and the degradation of detected metal ions was tested. The experiment demonstrated an effective reduction in these metals.

Keywords Box–Behnken method · RSM analysis · Silver nanoparticles · Wastewater treatment · Pollutants

Introduction

The conservation of clean and fresh water is a significant global concern, and therefore, it is of paramount importance to treat wastewater for reuse. Wastewater frequently contains contaminants that, if released into the water without treatment, can contaminate the water and infect aquatic organisms (Roy et al. 2019). Abdolalian and Taghavijeloudar 2022 posit that there are two primary sources of wastewater contamination: (i) Natural phenomena, including volcanic activity, soil erosion, and rock weathering; and (ii) human activities, such as mining, landfill operations, municipal runoff,

power lines and coatings, agriculture, and fuel combustion. The presence of a multitude of toxic inorganic and organic contaminants in wastewater from various sources, including agricultural, industrial, and domestic sectors, poses a significant threat to the environment and human health. These contaminants include heavy metals, excess nutrients, and pigments (Akpomie et al. 2022). Among the heavy metals (potentially toxic elements or PTEs) and metalloids, PTE belongs to the group of trace elements with different densities. The following elements are among the most prevalent in the list: copper (Cu), mercury (Hg), cadmium (Cd), zinc (Zn), tin (Sn), iron (Fe), lead (Pb), silver (Ag), manganese (Mn), chromium (Cr), cobalt (Co), arsenic (As), aluminium (Al), and nickel (Ni) waste (Kulal and Badalamoole 2020), (Obayomi et al. 2021). Consequently, these substances enter the human food chain and exert a deleterious effect on human health. The current focus is on the development of cost-effective adsorbents derived from readily accessible and inexpensive natural resources, including fruit peel, rice

✉ V. Gowthami
gowthami.sbs@vistas.ac.in

¹ Department of Physics, School of Basic Science, Vels Institute of Science Technology and Advanced Studies, Tamil Nadu, Pallavaram, Chennai 600117, India

husks, wheat straw, coconut and coffee waste, shells, mud, sugarcane bagasse, peat, agricultural waste, and household. Orange residue is a type of citrus fruit residue made up of peel and pulp (the juice-screening fraction), cellulose, pectin (galacturonic acid), hemicelluloses, lignin, chlorophyll pigments, and other low molecular weight substances, such as limonene, make up the majority of it (Pechyen et al. 2021; Podurets et al. 2022). The usage of orange peels in adsorption processes is known from the literature to be an agro-industrial by-product having adsorptive qualities (Premkumar et al. 2018; Roy et al. 2019). Bananas (*Musa Cavendish*) constitute a further fruit that is widely available on the market. The banana peel, which is typically discarded as general waste in landfill, remains behind since the banana itself is usually consumed or used to make other culinary products (Sanakousar et al. 2022). The potential use of banana peel as a functional component or preservative agent in the food industry has been suggested in the light of the recent discovery that it possesses significant antioxidant and antibacterial capabilities (Singh et al. 2023). Banana peel is naturally abundant in polymers including pectin and hemicellulose, and it was employed in the synthesis of AgNPs (Tan et al. 2021). Real-world analytical studies were conducted using wastewater that was gathered from Chengalpattu district, Tamil Nadu, India.

The present paper offers an in-depth examination of the wastewater research on an array of fruit peel-induced nanomaterials for sustainable wastewater management. It is intended to provide a valuable resource for the scientific and engineering communities engaged in wastewater research and treatment. Also, this research proposes the valorisation of agro-industrial biowaste offers significant potential benefits when considered in the context of the fundamental principles of green chemistry, the circular economy, nexus thinking, sustainability, and zero-cost and zero-waste manufacturing approaches.

Methodology

Synthesis of silver nanoparticles

The dried peels were ground to a powder. Aqueous extracts of each sample were prepared by adding water to the powder at a ratio of 10:1 (w:v). To inactivate the enzymes, the mixtures were immediately heated at 100 °C for 10 min. The mixtures were filtered through Whatman #1 filter paper, and the supernatants were saved for use in the preparation of AgNPs. Subsequently, 10 ml of plant extract and 90 ml of 1 mM silver nitrate (AgNO_3) solution were mixed in a flask for the preparation of AgNP. A stable dark colour was obtained after 24 h of storage at room temperature and in the dark. pH is adjusted by adding suitable concentration of

NaOH (0.1 M) in the prepared solutions in different conical flasks. Nanoparticle drying is employed to enhance their stability, particularly for long-term storage. The produced nanoparticles are kept in 2–8 °C for storage and future use.

Characterisation of nanoparticles

The AgNPs were characterised by a UV–vis spectrophotometer (GENESYS 10 s) for peak absorbance and surface plasmon resonance wavelength. The shape and morphology of prepared nanoparticles were obtained by FESEM. Particle size is calculated with the FESEM images.

Wastewater collection

Wastewater for the analysis was collected from Chengalpattu district, Tamil Nadu, India. A 7500 inductively coupled plasma mass spectrometer (ICPMS) was used to find the metal concentration present in the wastewater (APHA 3rd edition 2017). Using Box–Behnken method, an experimental design was produced to analyse metals like Al, Cu, and Zn as an initial sample experiment for optimising parameters.

Removal efficiency

The removal of metals was investigated by adding different adsorbent dosages of different pHs for definite time interval. Removal efficiency is calculated using given equation

$$\text{Removal efficiency (\%)} = \frac{A_0 - A_t}{A_0} \times 100\% \quad (1)$$

where A_0 is the initial metal concentration, and A_t is the final metal concentration.

Experimental design

A three-level Box–Behnken experimental design along with response surface modelling and quadratic programming were used to identify the ideal conditions for maximising the adsorption of metals by combined peel extract generated silver nanoparticles. A Box–Behnken design was employed in single-factor experiments to determine the effects of pH, contact time, and adsorbent quantity on the adsorption of metals on to nanoparticles. RSM furnished a final equation in terms of actual factors. Regression analysis was used to fit an experimental dataset with a second-order polynomial model. Using Design-Expert software, RSM and data analysis were performed. In Erlenmeyer flasks, all adsorption studies were carried out with synthetic contact period (10–180 min), and adsorbent mass (0.1–1 g) were investigated. Filtration was used to

remove the adsorbent from the samples, and then ICPMS was used to analyse the filtrate. The experiment's design is presented in Table 1 together with the initial parameters for the metals Al, Zn, and Cu. The pH range of 5–8 has been selected for study because it encompasses the acidic and basic natures of the interaction between silver nanoparticles.

Result and discussion

Synthesis of silver nanoparticles

Figure 1 shows the result from the reduction of CPE during the production of AgNPs. Nanoparticle production is indicated by a yellowish to brown colour change in the solution. Numerous researches have revealed conclusions that are similar to the colour change of solution to dark brown which confirm the presence of nanoparticles (Waghchaure et al. 2022). According to Waseem et al. 2023, the reduction of aqueous Ag⁺ ions into AgNPs and SPR caused the change in colour.

Table 1 Variable conditions of independent parameters for the experiment

Variables	Coded levels		
	– 1	0	1
pH	5	6.5	8
Adsorbent dosage g/mL	.1	.55	1
Contact time (min)	5	92.5	180

Characterisation analysis

The microstructure of combined peel extract-induced silver nanoparticles was examined using the FESEM instrument. Figure 2 depicts the shape of the nanoparticle conditions for CPE-AgNPs. The microstructure is in a spherical scattered structure, as demonstrated by the FESEM study. The CPE-AgNPs surface has particles that are present in small sizes with good particle dispersion, which significantly increases the CPE-AgNPs effective surface area. According to the FESEM micrograph, the particles were made up of grains with diameters of 37.9 nm, both coarse and fine. The homogeneity, form, and small size particles present in the CPE biosorbent were validated by SEM examination (Huo et al. 2023). UV–visible spectra exhibited a peak absorbance and SPR wavelength at 438 nm in Fig. 2. Huo et al. (2023) confirmed the presence of SPR resonance in the same region.

Wastewater analysis

The collected wastewater was analysed, and metal contents are traced in Table 2. The analysis showed that the metals mainly aluminium, copper and zinc are showing desirable quantity in per litre of water. To optimise the parameters, initial experiments were done with these three metals separately using RSM analysis.

Model evaluation and optimisation

RSM with a Box–Behnken design and ANOVA was used for adsorption on CPE-AgNPs. The conditions and the results of metal adsorption are shown in Table 3, respectively. The Model F-value of Al (474.77), Cu (252.78), and Zn (173.36) implies that the model is significant. There is only a 0.01%

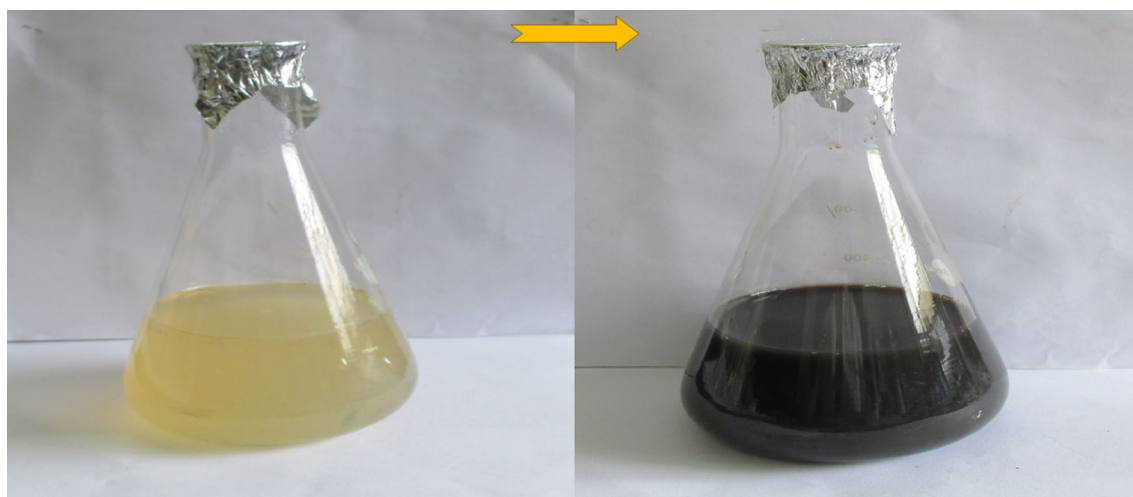


Fig. 1 Change of colour of CPE-AgNO₃ solution after formation nanoparticles

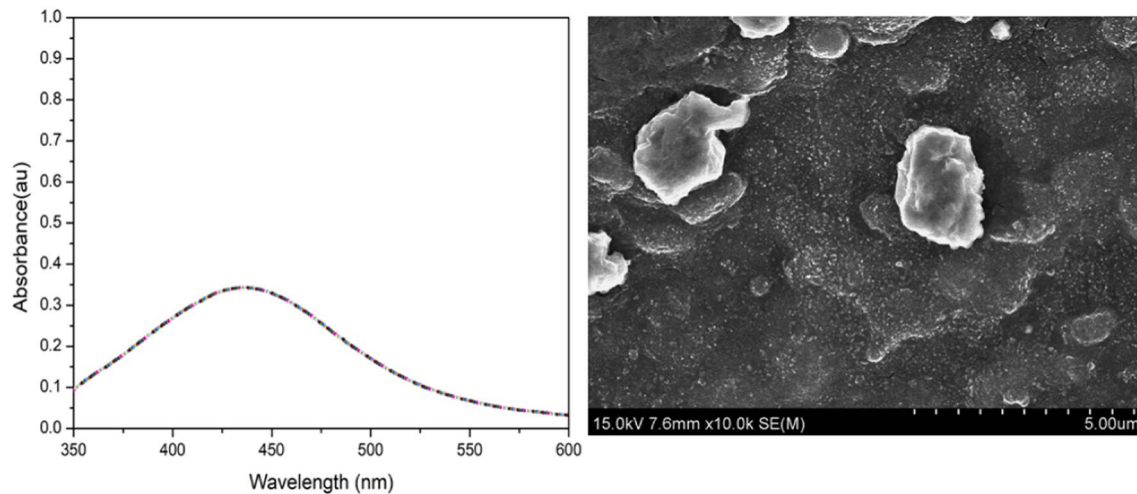


Fig. 2 FESEM images of prepared CPE-AgNPs and UV-vis spectra of CPE-AgNPs

Table 2 Metal detection in collected wastewater before treatment

Sl. no.	Test parameters	Results (mg/L)
1	Silver (Ag)	BDL(DL:.001)
2	Aluminium (Al)	0.675
3	Arsenic (As)	BDL(DL:.001)
4	Boron (B)	0.132
5	Barium (Ba)	0.270
6	Cadmium (Cd)	BDL(DL:.001)
7	Cobalt (Co)	BDL(DL:.001)
8	Chromium (Cr)	0.010
9	Copper (Cu)	0.278
10	Manganese (Mn)	0.057
11	Nickel (Ni)	0.020
12	Lead (Pb)	0.029
13	Selenium (Se)	BDL(DL:.001)
14	Zinc (Zn)	0.519
15	Molybdenum (Mo)	BDL(DL:.001)
16	Antimony (Sb)	BDL(DL:.001)
17	Uranium (U)	BDL(DL:.001)

chance that a F-value this large could occur due to noise. P-values less than 0.0500 indicate model terms are significant (Berkani et al. 2020). In this case B, C, AB, AC, BC, A^2 , B^2 , and C^2 are significant model terms. Because the model coefficient (R^2) for Al (0.9984), Cu (0.9996), and Zn (0.9955), it can be said that 99.84% for Al, 99.96% for Cu, and 99.55% for Zn of the model-predicted values matched the experimental values on nano-adsorption by synthesised CPE-AgNPs as shown in Table 4. For aluminium adsorption, the Lack of Fit F-value of 123.24 implies the Lack of Fit is significant. There is only a 0.02% chance that a Lack of Fit F-value this large could occur due to noise. For copper

adsorption, the Lack of Fit F-value of 6.77 implies the Lack of Fit is significant. There is only a 4.79% chance that a Lack of Fit F-value this large could occur due to noise. And for zinc adsorption, the Lack of Fit F-value of 44.68 implies the Lack of Fit is significant. There is only a 0.16% chance that a Lack of Fit F-value this large could occur due to noise, but Box–Behnken designs are not an optimal choice when the objective is to elicit responses at the extremes.

For aluminium,

$$f = 0.0917 - 0.0008A + 0.0048B + 0.0118C - 0.0083AB - 0.0053AC + 0.0082BC - 0.0179A^2 - 0.0166B^2 - 0.0173C^2 \quad (2)$$

For copper,

$$f = 0.0917 - 0.0007A + 0.0060B + 0.0123C - 0.0065AB - 0.0050AC + 0.0095BC - 0.0193A^2 - 0.0164B^2 - 0.0164C^2 \quad (3)$$

For zinc,

$$f = 0.0831 - 0.0006A + 0.0040B + 0.0121C - 0.0065AB - 0.0048AC + 0.0125BC - 0.0193A^2 - 0.0155B^2 - 0.0150C^2 \quad (4)$$

Response surface methodology (RSM) analysis

Two-dimensional (2D) contour plots and three-dimensional (3D) response surface graphs were made because they are useful in determining maximum, minimum, and middle response points. With contour plots Fig. 3, the levels of the variables can be determined and also contribute to a desired response (Pambi and Musonge 2016, Mohamad et al. 2019). In addition, the variable levels are plotted in a curve with equal response. Because of these reasons, contour plots are easier to interpret. Figures 4, 5, 6, and 7 show the effect of

Table 3 Experimental and predicted values of aluminium, copper and zinc adsorption on CPE-AgNPs

Run	Factor 1	Factor 2	Factor 3	Response Al (g/mL)		Response Cu (g/mL)		Response Zn (g/mL)	
	pH	Contact time (min)	Adsorbent amount (g/ml)	Actual value	Predicted value	Actual value	Predicted value	Actual value	Predicted value
1	6.5	5	0.1	0.0509	0.0494	0.0507	0.0494	0.0507	0.0507
2	6.5	180	0.1	0.0423	0.0427	0.0428	0.0427	0.0428	0.0426
3	5	180	0.55	0.0713	0.0704	0.0703	0.0704	0.0703	0.0704
4	8	92.5	0.1	0.0494	0.0500	0.0486	0.0500	0.0486	0.0487
5	5	92.5	0.1	0.0389	0.0395	0.0387	0.0395	0.0387	0.0388
6	8	5	0.55	0.0598	0.0607	0.0595	0.0607	0.0595	0.0594
7	6.5	92.5	0.55	0.0917	0.0917	0.0918	0.0917	0.0918	0.0918
8	6.5	92.5	0.55	0.0920	0.0917	0.0917	0.0917	0.0917	0.0918
9	5	5	0.55	0.0432	0.0442	0.0443	0.0442	0.0443	0.0442
10	6.5	92.5	0.55	0.0916	0.0917	0.0917	0.0917	0.0917	0.0918
11	6.5	92.5	0.55	0.0917	0.0917	0.0916	0.0917	0.0916	0.0918
12	6.5	180	1	0.0810	0.0825	0.0862	0.0825	0.0862	0.0864
13	8	180	0.55	0.0547	0.0537	0.0548	0.0537	0.0548	0.0549
14	6.5	5	1	0.0570	0.0566	0.0561	0.0566	0.0561	0.0563
15	8	92.5	1	0.0636	0.0630	0.0507	0.0630	0.0633	0.0507
16	6.5	92.5	0.55	0.0916	0.0917	0.0428	0.0917	0.0915	0.0426
17	5	92.5	1	0.0742	0.0736	0.0703	0.0736	0.0735	0.0704

pH and contact time on aluminium, copper, and zinc adsorption by CPE-AgNPs. The adsorbed copper amount increased with an increase in pH until it reaches a plateau at 5, indicating that there are further improvements for metal levels. At the same time, contact time has important effects on metal's adsorption on the adsorbent. As a result, the impact of pH on the metal adsorption level was more significant than of contact time. The optimised parameters of this experiment which we obtained is pH = 5, contact time is 92.5 min, and adsorbent dosage is 0.1 g.

Analytical application to real sample

The analytical applicability of a new adsorbent was tested for the removal of these metals from wastewater samples obtained from Chengalpattu district, Tamil Nadu, India. The developed analytical method uses the Box–Behnken experimental design in combination with the response surface modelling (RSM) and quadratic programming. An effective and eco-friendly adsorbent, the CPE-AgNPs was applied to various real samples. Adsorption is defined as a chemical process which involves the removal of pollutants from wastewater by the trapping of these pollutants in the pore structure of an adsorbent material. The process is widely utilised in wastewater treatment due to its simplicity, efficiency, and cost-effectiveness. The adsorbent, comprising silver nanoparticles (AgNPs), is a crucial component of the adsorption process. Adsorptive materials

can capture pollutant molecules on their surface and possess porosity and insolubility in water. The pollutants, or adsorbates, that are removed from wastewater are referred to as the adsorbate. Adsorbent dosage of 0.1 g with different pH was prepared. The solutions were agitated with 0.1 g of CPE-AgNPs at a shaking speed of about 150 rpm for 92.5 min. The results in Fig. 8 clearly show the efficiency of CPE-AgNPs for the removal of these ions from wastewater with optimised parameter obtained using the standard additions method. The efficiency of the adsorption is calculated (Eq. 1) for each pH (Tables 5, 6), and a bar chart is plotted for each metals as shown in Fig. 8. Silver nanoparticles (AgNPs) have the capacity to adsorb a range of substances through a number of mechanisms, including electrostatic adsorption, agglomeration precipitation, oxidation and sulphurisation, ion exchange, and weak interaction. Electrostatic adsorption is the attraction of charged particles or molecules to a surface with an opposite charge due to electrostatic interaction. Agglomeration describes the process of particles colliding and sticking together to form larger particles. Oxidation is the addition of oxygen to a substance or the loss of electrons from one element and the gain of electrons by another. Oxidation and reduction reactions occur concurrently in chemical reactions. Ion exchange systems remove dissolved ions from aqueous systems using ion exchangers. Lung et al. (2018) studied removal of Pb and Cd from aqueous solution with maximum monolayer adsorption capacity (q_{\max}) of 13.50 mg g⁻¹ and 12.03 mg g⁻¹ for the two metal

Table 4 Analysis of variance (ANOVA) results of response surface for aluminium, copper, and zinc adsorption

Source	df	Sum of squares			Mean square			F-value			P value		
		Al	Cu	Zn	Al	Cu	Zn	Al	Cu	Zn	Al	Cu	Zn
Model	9	0.0062	0.0063	0.0063	0.0007	0.0007	0.0009	474.77	25,278.24	25,278.24	<0.0001	<0.0001	<0.0001
A-pH	1	1.250E-09	4.500E-08	4.500E-08	1.250E-09	4.500E-08	3.125E-06	0.0009	1.62	1.62	0.9773	0.2438	0.4662
B-Contact time	1	0.0002	0.0002	0.0002	0.0002	0.0002	0.0001	127.87	8512.69	8512.69	<0.0001	<0.0001	0.0018
C-Adsorbent amount	1	0.0011	0.0012	0.0012	0.0011	0.0012	0.0012	771.11	43,470.58	43,470.58	<0.0001	<0.0001	<0.0001
AB	1	0.0003	0.0002	0.0002	0.0003	0.0002	0.0002	191.16	8479.99	8479.99	<0.0001	<0.0001	0.0007
AC	1	0.0001	0.0001	0.0001	0.0001	0.0001	0.0001	77.21	3635.05	3635.05	<0.0001	<0.0001	0.0040
BC	1	0.0003	0.0004	0.0004	0.0003	0.0004	0.0006	184.31	12,992.29	12,992.29	<0.0001	<0.0001	<0.0001
A ²	1	0.0013	0.0015	0.0015	0.0013	0.0015	0.0023	933.02	53,103.91	53,103.91	<0.0001	<0.0001	<0.0001
B ²	1	0.0012	0.0011	0.0011	0.0012	0.0011	0.0016	804.65	37,805.42	37,805.42	<0.0001	<0.0001	<0.0001
C ²	1	0.0013	0.0012	0.0012	0.0013	0.0012	0.0015	876.48	43,768.05	43,768.05	<0.0001	<0.0001	<0.0001
Residual	7	0.0000	1.945E-07	1.945E-07	1.442E-06	2.779E-08	5.265E-06						
Lack of Fit	3	9.983E-06	1.625E-07	1.625E-07	3.328E-06	5.417E-08	0.0000	123.24	1.62	1.62	0.0002	0.0479	0.0016
Pure Error	4	1.080E-07	3.200E-08	3.200E-08	2.700E-08	8.000E-09	2.670E-07	474.77	8512.69	8512.69	<0.0001	<0.0001	<0.0001
Cor Total	16	0.0062	0.0063	0.0063	0.0007	0.0007	0.0009	0.0009	43,470.58	43,470.58	<0.0001	<0.0001	0.4662

ions, with banana peel as nanoadsorbent for heavy metals using the batch adsorption technique and obtained about 99% removal percentage for Pb.

Conclusion

This study explores the CPE-AgNPs as a new, effective, and inexpensive adsorbent and an alternative to costly adsorbents for the removal of metal ions (Al, Cu, and Zn) from wastewater solutions. A batch experimental system was used to investigate the feasibility of this naturally synthesised nanoadsorbent as a possible adsorbent for these metals from the aqueous medium by using the response surface methodological (RSM) and Box–Behnken design approach. The results prove that this method is an efficient technique for studying the influence of major process parameters on response factor by significantly reducing the number of experiments and hence providing optimum conditions. CPE-AgNPs was found suitable for removal of aluminium, copper, and zinc from aqueous solution. The CPE-AgNPs is low cost and eco-friendly with high sorption capacity values that are considered among the main advantages. This adsorbent has been shown to have comparable performance with commercial levels. SEM and UV-visible analysis confirmed the presence of nanoparticles with SPR resonance at 438 nm. SEM micrographs were analysed before and after adsorption. With response surface methodology, parameters are optimised and analysed in real-world experiments. The parameters optimised showed an average of eighty percentage good adsorption efficiency. Nevertheless, the threat of nanoparticles being released into the environment and their toxicity to aquatic and terrestrial and terrestrial biological systems at low concentrations are well understood with recent research. Furthermore, the applications of silver nanoparticles in dye effluent treatment technologies require full risk assessments and environmental health and safety studies are also limited. It is therefore crucial to assess the toxicity of silver nanoparticles and the risks associated with the use of application of silver nanoparticles in dye effluent treatment. Research on in vivo immunotoxicity, the influence of nanomaterial shape on toxicity and the detailed study of the adsorption kinetics of silver nanoparticles on different biological macromolecules are still in their infancy.

Fig. 3 Contour plots for adsorption of Al, Cu, and Zn on CPE-AgNPs

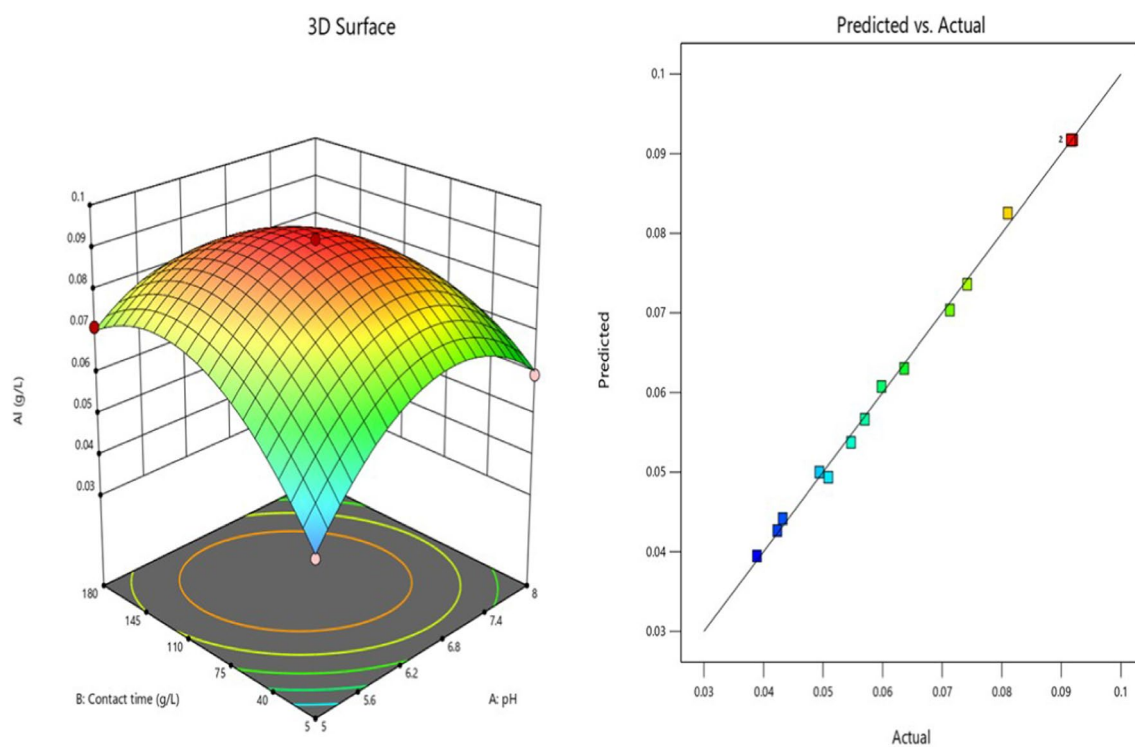
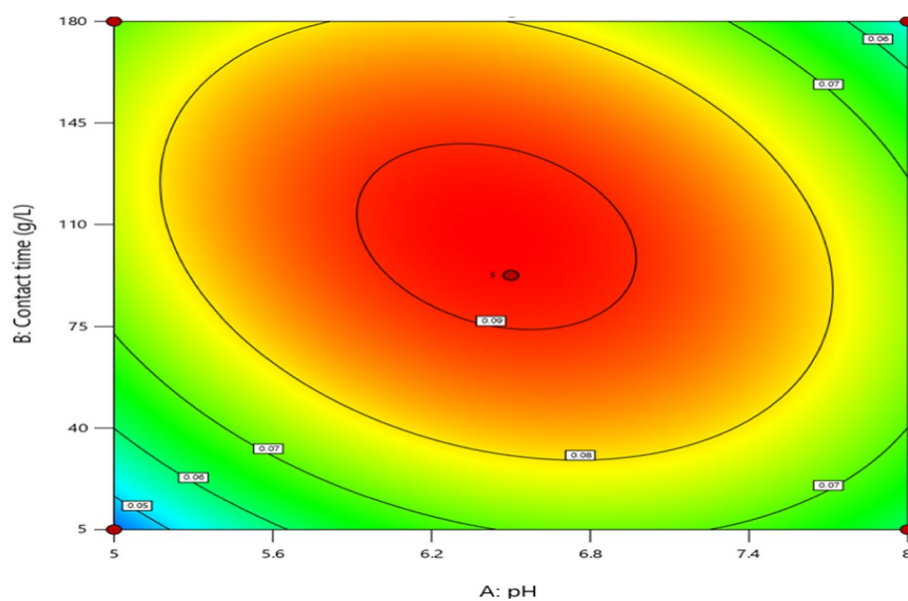


Fig. 4 3D surface graphs of aluminium adsorption and predicted plots

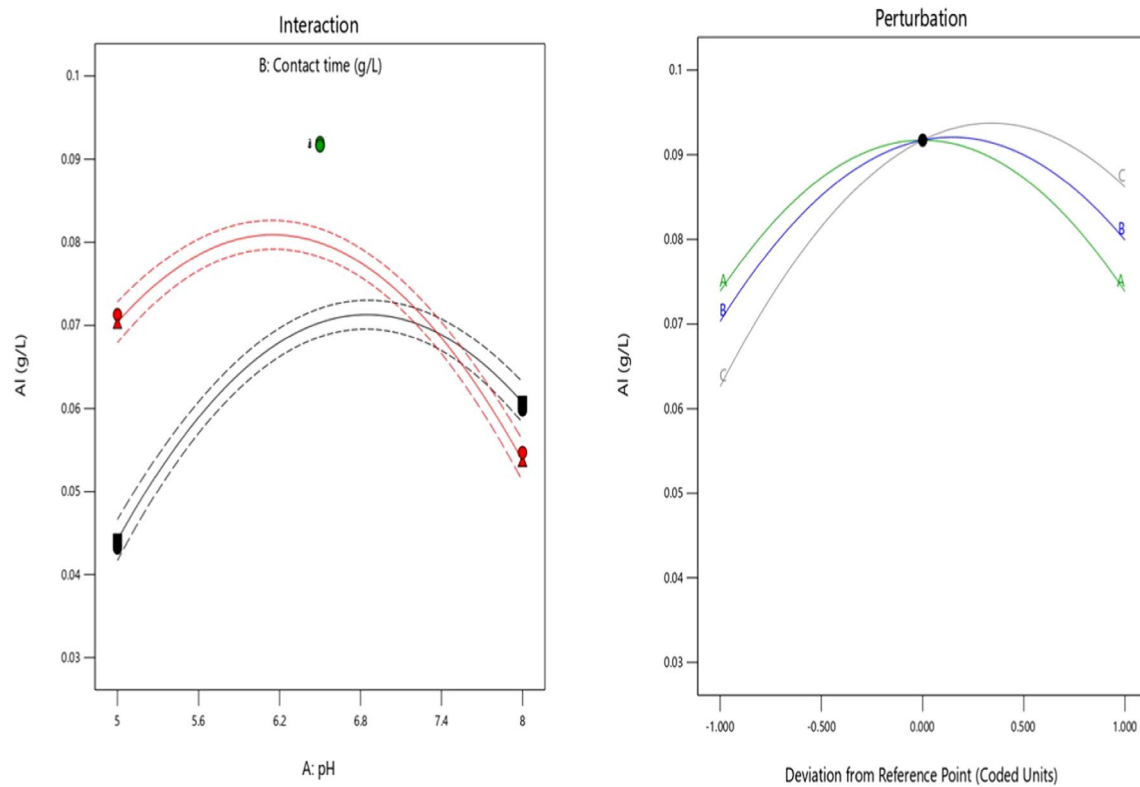


Fig. 5 Graphs of aluminium adsorption with interaction and perturbation plots

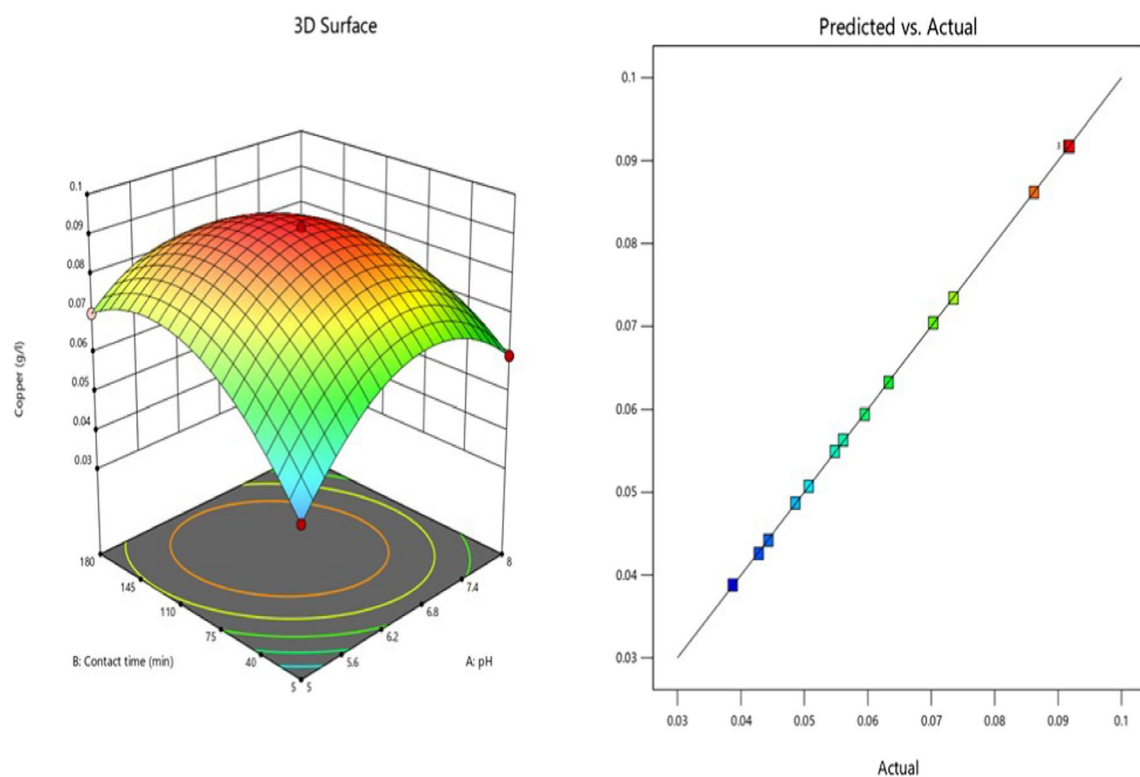


Fig. 6 Response surface graphs of copper adsorption and predicted plots

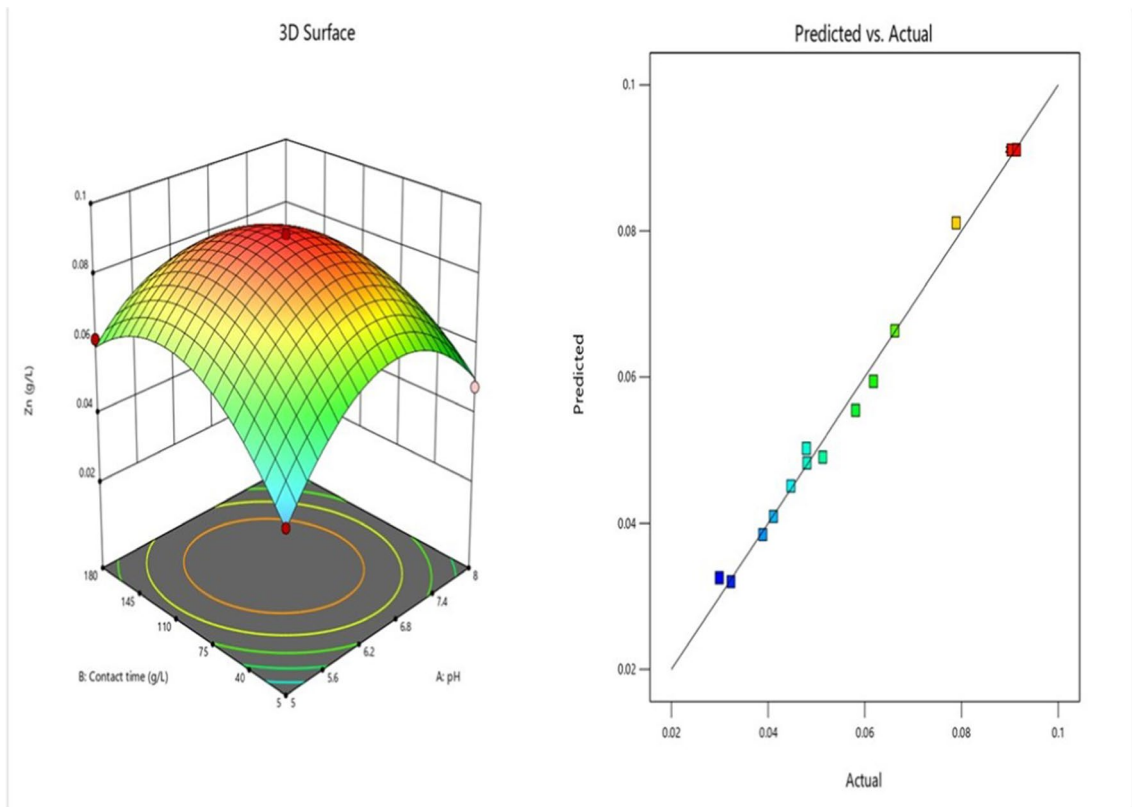


Fig. 7 Response surface graphs of zinc adsorption and predicted plots

Fig. 8 Calculated percentage efficiency of different metals after adsorption

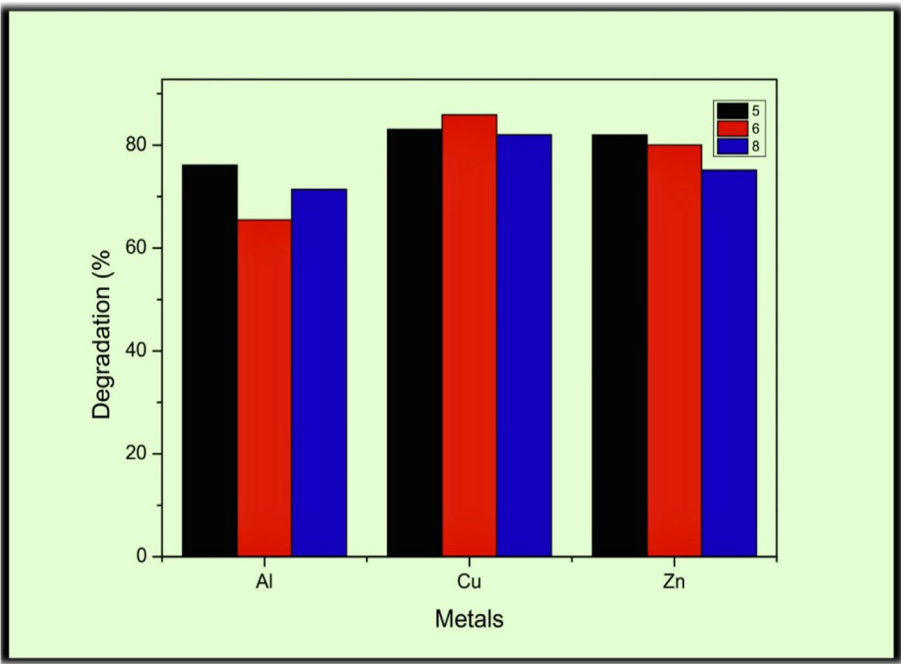


Table 5 Metal analysis after the treatment with nanoparticles using ICPMS

	pH		
	5	6	8
Al (Control-.675)	0.161	0.233	0.193
Cu (Control-.278)	0.047	0.039	0.050
Zn (Control-.519)	0.095	0.102	0.129

Table 6 Calculated efficiency of different metals after adsorption

	pH		
	5	6	8
Al	76.1%	65.48%	71.40%
Cu	83.09%	85.9%	82.01%
Zn	82%	80.03%	75.14%

Acknowledgements The authors thank all the experts of the Vels Institute of Science Technology and Advanced Studies, Chennai, for their resilience in this research.

Author contributions Jyolsna P done the conceptualization and design involved in this work, prepared the materials, and wrote the first draft of the manuscript. Data collection was presented by Hajeera Aseen A. Supervision and validation of the data were carried out by Gowthami V. All other authors provided feedback on earlier drafts. The final manuscript was read and approved by all writers.

Funding No funding was received.

Declarations

Conflict of interest The authors have no competing interests to disclose.

Open Access This article is licensed under a Creative Commons Attribution-NonCommercial-NoDerivatives 4.0 International License, which permits any non-commercial use, sharing, distribution and reproduction in any medium or format, as long as you give appropriate credit to the original author(s) and the source, provide a link to the Creative Commons licence, and indicate if you modified the licensed material. You do not have permission under this licence to share adapted material derived from this article or parts of it. The images or other third party material in this article are included in the article's Creative Commons licence, unless indicated otherwise in a credit line to the material. If material is not included in the article's Creative Commons licence and your intended use is not permitted by statutory regulation or exceeds the permitted use, you will need to obtain permission directly from the copyright holder. To view a copy of this licence, visit <http://creativecommons.org/licenses/by-nc-nd/4.0/>.

References

Abdolalian S, Taghaviyeloudar M (2022) Performance evaluation and optimization of ZnO-PVP nanoparticles for photocatalytic wastewater treatment: interactions between UV light intensity and

nanoparticles dosage. *J Clean Prod* 365:132833. <https://doi.org/10.1016/j.jclepro.2022.132833>

Ahmed A, Usman M, Ji Z, Rafiq M, Yu B, Shen Y, Cong H (2023) Nature-inspired biogenic synthesis of silver nanoparticles for antibacterial applications. *Mater Today Chem* 27:101339. <https://doi.org/10.1016/j.mtchem.2022.101339>

Akpomie KG, Adegoke KA, Oyedotun KO, Ighalo JO, Amaku JF, Olisah C, Adeola AO, Iwuozor KO, Conradie J (2022) Removal of bromophenol blue dye from water onto biomass, activated carbon, biochar, polymer, nanoparticle, and composite adsorbents. *Biomass Convers Biorefin.* <https://doi.org/10.1007/s13399-022-03592-w>

Aliero AS, Hasmoni SH, Haruna A, Isah M, Malek NNN, Zawawi NA (2024) Bibliometric exploration of green synthesized silver nanoparticles for antibacterial activity. *Emerg Contam.* <https://doi.org/10.1016/j.emcon.2024.100411>

Berkani M, Kadmi Y, Bouchareb MK, Bouhelassa M, Bouzaza A (2020) Combination of a Box-Behnken design technique with response surface methodology for optimization of the photocatalytic mineralization of CI Basic Red 46 dye from aqueous solution. *Arab J Chem* 13(11):8338–8346. <https://doi.org/10.1016/j.arabjc.2020.05.013>

Bogireddy NKR, Kumar HK, Mandal BK (2015) Biofabricated silver nanoparticles as green catalyst in the degradation of different textile dyes. *J Environ Chem Eng* 4(1):56–64. <https://doi.org/10.1016/j.jece.2015.11.004>

Huo Y, Xiu S, Meng L, Quan B (2023) Solvothermal synthesis and applications of micro/nano carbons: A review. *Chem Eng J* 451:138572. <https://doi.org/10.1016/j.cej.2022.138572>

Kulal P, Badalamoole V (2020) Efficient removal of dyes and heavy metal ions from waste water using Gum ghatti – graft – poly(4-acryloylmorpholine) hydrogel incorporated with magnetite nanoparticles. *J Environ Chem Eng* 8(5):104207. <https://doi.org/10.1016/j.jece.2020.104207>

Liu L, Yu C, Ahmad S, Ri C, Tang J (2023) Preferential role of distinct phytochemicals in biosynthesis and antibacterial activity of silver nanoparticles. *J Environ Manage* 344:118546. <https://doi.org/10.1016/j.jenvman.2023.118546>

Lung I, Stan M, Opris O, Soran M, Senila M, Stefan M (2018) Removal of Lead(II), Cadmium(II), and Arsenic(III) from Aqueous Solution Using Magnetite Nanoparticles Prepared by Green Synthesis with Box–Behnken Design. *Anal Lett* 51(16):2519–2531. <https://doi.org/10.1080/00032719.2018.1446974>

Mohammed AM, Hassan KT, Hassan OM (2023) Assessment of antimicrobial activity of chitosan/silver nanoparticles hydrogel and cryogel microspheres. *Int J Biol Macromol* 233:123580. <https://doi.org/10.1016/j.ijbiomac.2023.123580>

Moraes LC, Gomes MP, Ribeiro-Andrade R, Garcia QS, Figueredo CC (2023) Green synthesized silver nanoparticles for iron and manganese ion removal from aqueous solutions. *Environ Pollut* 327:121483. <https://doi.org/10.1016/j.envpol.2023.121483>

Obayomi KS, Oluwadiya AE, Lau SY, Dada AO, Akubuo-Casmir D, Adelani-Akande TA, Bari AF, Temidayo SO, Rahman MM (2021) Biosynthesis of Tithonia diversifolia leaf mediated Zinc Oxide Nanoparticles loaded with flamboyant pods (*Delonix regia*) for the treatment of Methylene Blue Wastewater. *Arab J Chem* 14(10):103363. <https://doi.org/10.1016/j.arabjc.2021.103363>

Pambi RLL, Musonge P (2016) Application of response surface methodology (RSM) in the treatment of final effluent from the sugar industry using Chitosan. *WIT Trans Ecol Environ.* <https://doi.org/10.2495/wp160191>

Pechyen C, Ponsanti K, Tangnorawich B, Ngernyuan N (2021) Waste fruit peel – Mediated green synthesis of biocompatible gold nanoparticles. *J Mater Res Technol* 14:2982–2991. <https://doi.org/10.1016/j.jmrt.2021.08.111>

- Podurets A, Odegova V, Cherkashina K, Bulatov A, Bobrysheva N, Osmolowsky M, Voznesenskiy M, Osmolovskaya O (2022) The strategy for organic dye and antibiotic photocatalytic removal for water remediation in an example of Co-SnO₂ nanoparticles. *J Hazard Mater* 436:129035. <https://doi.org/10.1016/j.jhazmat.2022.129035>
- Premkumar K, Vinod E, Sathishkumar S, Pulimood AB, Umaefulam V, Samuel PP, John TA (2018) Selfdirected learning readiness of Indian medical students: a mixed method study. *BMC Med Edu* 18(1). <https://doi.org/10.1186/s12909-018-1244-9>
- Roy A, Bulut O, Some S, Mandal AK, Yilmaz MD (2019) Green synthesis of silver nanoparticles: biomolecule-nanoparticle organizations targeting antimicrobial activity. *RSC Adv* 9(15):2673–2702. <https://doi.org/10.1039/C8RA08982E>
- Sanakousar F, Vidyasagar C, Jiménez-Pérez V, Prakash K (2022) Recent progress on visible-light-driven metal and non-metal doped ZnO nanostructures for photocatalytic degradation of organic pollutants. *Mater Sci Semicond Process* 140:106390. <https://doi.org/10.1016/j.mssp.2021.106390>
- Singh AK, Chaubey AK, Kaur I (2023) Remediation of water contaminated with antibiotics using biochar modified with layered double hydroxide: Preparation and performance. *J Hazard Mater Adv* 10:100286. <https://doi.org/10.1016/j.hazadv.2023.100286>
- Subha T, Srilatha M, Naveen P, Thirumalaisamy R (2024) Green synthesis characterization and optimization of silver nanoparticles from carica papaya using box behnken design and its activity against dental caries causing streptococcus sp. *Chem Data Collect*. <https://doi.org/10.1016/j.cdc.2024.101139>
- Tan KB, Sun D, Huang J, Odoom-Wubah T, Li Q (2021) State of arts on the bio-synthesis of noble metal nanoparticles and their biological application. *Chin J Chem Eng* 30:272–290. <https://doi.org/10.1016/j.cjche.2020.11.010>
- Thi TUD, Nguyen TT, Thi YD, Thi KHT, Phan BT, Pham KN (2020) Green synthesis of ZnO nanoparticles using orange fruit peel extract for antibacterial activities. *RSC Adv* 10(40):23899–23907. <https://doi.org/10.1039/d0ra04926c>
- Vadakkan K, Rumjit NP, Ngangbam AK, Vijayanand S, Nedumpillil NK (2024) Novel advancements in the sustainable green synthesis approach of silver nanoparticles (AgNPs) for antibacterial therapeutic applications. *Coord Chem Rev* 499:215528
- Waghchaure RH, Adole VA, Jagdale BS (2022) Photocatalytic degradation of methylene blue, rhodamine B, methyl orange and Eriochrome black T dyes by modified ZnO nanocatalysts: A concise review. *Inorg Chem Commun* 143:109764. <https://doi.org/10.1016/j.inoche.2022.109764>
- Waseem S, Sittar T, Kayani ZN, Gillani S, Rafique M, Nawaz MA, Shaheen SM, Assiri MA (2023) Plant mediated green synthesis of zinc oxide nanoparticles using Citrus jambhiri lushi leaves extract for photodegradation of methylene blue dye. *Phys B Condensed Matter* 663:415005. <https://doi.org/10.1016/j.physb.2023.415005>

Publisher's Note Springer Nature remains neutral with regard to jurisdictional claims in published maps and institutional affiliations.